

q-VAE for Disentangled Representation Learning and Latent Dynamical Systems

Taisuke Kobayashi¹

Abstract—This paper proposes a novel variational autoencoder (VAE) derived from Tsallis statistics, named q-VAE. A vanilla VAE is utilized to statistically extract latent space hidden in data sampled. Such latent space is useful to make robots controllable in feasible computational time and cost. To improve usefulness of the latent space, this paper focuses on disentangled representation learning like β -VAE, which is the baseline for it. Starting from the viewpoint of Tsallis statistics, a new lower bound of the q-VAE is derived to maximize likelihood of the data sampled. This can be regarded as an adaptive β -VAE with a deformed Kullback-Leibler divergence. To verify benefits from the q-VAE, a benchmark task to extract the latent space from MNIST dataset is performed. It is found that the q-VAE improved the disentangled representation while not deteriorating reconstruction accuracy of the data. As another advantage of the q-VAE, it does not require independency between the data. This advantage is demonstrated in learning latent dynamics of a nonlinear dynamical simulation. By combining the disentangled representation, the q-VAE achieves stable and accurate long-term state prediction from the initial state and the actions at respective times.

Index Terms—Deep Learning in Robotics and Automation, Model Learning for Control

I. INTRODUCTION

Recently, deep learning [1] is getting the most powerful tool to resolve analytically unsolvable problems. In robotics and its control, several researches using the deep learning succeeded in achieving complicated tasks relying on raw images from cameras [2], [3]. The deep learning is however likely to require too numerous samples for end-to-end learning: from extracting features hidden in inputs (e.g., images) to optimal control based on the features.

Modularization of functions, such as extracting the features [4], [5] and the optimal control [6], [7], is effective to reduce the number of samples. In particular, control theory has long been studied while discussing stability, convergence speed, and so on. Exploiting the conventional but powerful control technology is therefore one of solutions to reduce the number of samples, although the features extracted without ingenuity would not be suitable for that.

Hence, this paper focuses on methods to extract the features hidden in the inputs. To this end, a variational autoencoder (VAE) [4] is one of promising methods, which encodes the inputs to latent space with stochastic latent variables (and decodes them to the inputs) in an unsupervised manner. Actually, control methods on the latent space gained by the VAE have been proposed [8], [9].

To improve usefulness of the latent space, recent progress of the VAE has stepped into disentangled representation learning [10], which assigns independent attributes hidden in the inputs to the axes of the latent space without supervisory signals. However, a representative of this methodology, β -VAE [11], would lose value of the VAE as a data generation model due to deteriorating the reconstruction accuracy of the inputs. Although relatives of the β -VAE have been proposed to resolve this problem, they have drawbacks from the viewpoint of practicality: e.g., a heuristic design difficult to be optimized [12]; an assumption of batch data [13]; and optimization of an additional discriminator network [14].

Towards simple and low-cost but sufficiently practical disentangled representation learning, this paper tackles a novel derivation of the VAE combined with Tsallis statistics [15]–[17], which refers to the extended version of general statistics by given a real parameter q . This derivation, named q-VAE, mathematically gives us an adaptive β according to the amount of information in the latent variables. Thanks to the adaptive β , the q-VAE achieves proper extraction of the essential information of the inputs while maintaining the reconstruction accuracy of the inputs. In addition, deformed Kullback-Leibler (KL) divergence [17], [18] makes the magnitude of regularization in the vicinity of the center of prior weaker, which helps the latent space meaningful.

As another perspective, the q-VAE has an additional advantage, namely it allows the inputs non independent and identically distributed (i.i.d.), which is basically caused during controlling robots. In this paper, therefore, the q-VAE is simply extended to a model to learn latent dynamics of the inputs when giving manipulated variables. Using this, the latent variables encoded are transited to next ones that are decoded to the next inputs. Thanks to the disentangled representation, even if the latent dynamics model is constrained as a diagonal system (namely, latent variables are independent), the q-VAE would alleviate deterioration of prediction performance. In addition, such a simple dynamical system is easily exploited to control robots with low computational cost.

For verification of the q-VAE, a MNIST benchmark is first performed. From this benchmark, it is found that the q-VAE with an appropriate parameter outperforms the β -VAE (i.e., the fixed β) in terms of the disentangled representation and the reconstruction accuracy of the inputs. Furthermore, learning of the latent dynamics in a nonlinear simulation is performed. Although the conventional methods fail to predict future states stably, the q-VAE achieves the stable and accurate long-term state prediction from the initial state and actions at respective times.

¹Taisuke Kobayashi is with the Division of Information Science, Nara Institute of Science and Technology, 8916-5 Takayama-cho, Ikoma, Nara 630-0192, Japan kobayashi@is.naist.jp

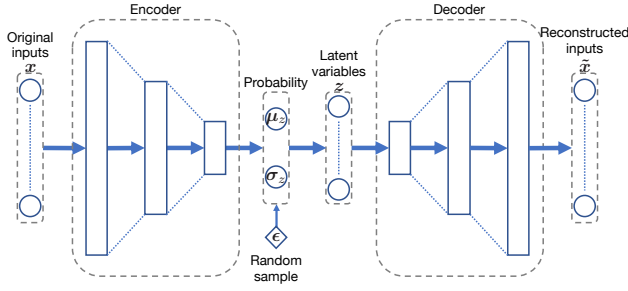


Fig. 1. Network structure of the VAE [4]: it encodes the inputs to the stochastic latent space with the specified size d ; the latent variables are sampled by reparameterization trick, and decoded to the inputs to be reconstructed; this structure is the same as the β -VAE [11] and the proposal, named the q -VAE.

II. PRELIMINARIES

A. Variational autoencoder: VAE

Let's briefly introduce the VAE [4] (see Fig. 1). Now, a generative model of inputs \mathbf{x} from latent variables \mathbf{z} is considered. Such a decoder is approximated by (deep) neural networks with parameters θ : $p(\mathbf{x} | \mathbf{z}; \theta)$. The VAE aims to maximize the log likelihood of the N inputs, $\log p(X)$ where $X = \{\mathbf{x}_1, \dots, \mathbf{x}_N\}$. Note that by assuming that the inputs are i.i.d., $\log p(X)$ can be simplified to the sum of respective log likelihoods $\sum_{n=1}^N \log p(\mathbf{x}_n)$. To maximize $\log p(X)$ indirectly, an evidence lower bound (ELBO) $\mathcal{L}(X)$, which is derived by using Jensen's inequality and an encoder with parameters ϕ , $\rho(\mathbf{z} | \mathbf{x}_n; \phi)$, is maximized. Now, $\mathcal{L}(X)$ is derived as follows:

$$\begin{aligned}
 \log p(X) &= \sum_{n=1}^N \log \int p(\mathbf{x}_n | \mathbf{z}; \theta) p(\mathbf{z}) d\mathbf{z} \\
 &= \sum_{n=1}^N \log \int \frac{\rho(\mathbf{z} | \mathbf{x}_n; \phi)}{\rho(\mathbf{z} | \mathbf{x}_n; \phi)} p(\mathbf{x}_n | \mathbf{z}; \theta) p(\mathbf{z}) d\mathbf{z} \\
 &\geq \sum_{n=1}^N \mathbb{E}_{\rho(\mathbf{z} | \mathbf{x}_n; \phi)} \left[\log \frac{p(\mathbf{x}_n | \mathbf{z}; \theta) p(\mathbf{z})}{\rho(\mathbf{z} | \mathbf{x}_n; \phi)} \right] \\
 &=: \mathcal{L}(X)
 \end{aligned} \tag{1}$$

where $p(\mathbf{z})$ is a prior of the latent variables. $\mathcal{L}(X)$ can be summarized as follows:

$$\begin{aligned}
 \mathcal{L}(X) &= \sum_{n=1}^N \mathbb{E}_{\rho(\mathbf{z} | \mathbf{x}_n; \phi)} [\log p(\mathbf{x}_n | \mathbf{z}; \theta)] \\
 &\quad - \text{KL}(\rho(\mathbf{z} | \mathbf{x}_n; \phi) || p(\mathbf{z})) \\
 &\simeq \sum_{n=1}^N \log p(\mathbf{x}_n | \mathbf{z}_n; \theta) - \text{KL}(\rho(\mathbf{z} | \mathbf{x}_n; \phi) || p(\mathbf{z}))
 \end{aligned} \tag{2}$$

The first term denotes the negative reconstruction error in the autoencoder and the second term, i.e., the KL divergence between the posterior and the prior, is the regularization term to try to $\mathbf{z} \sim p(\mathbf{z})$. In general, $p(\mathbf{z})$ is given as standard normal distribution $\mathcal{N}(\mathbf{0}, I)$.

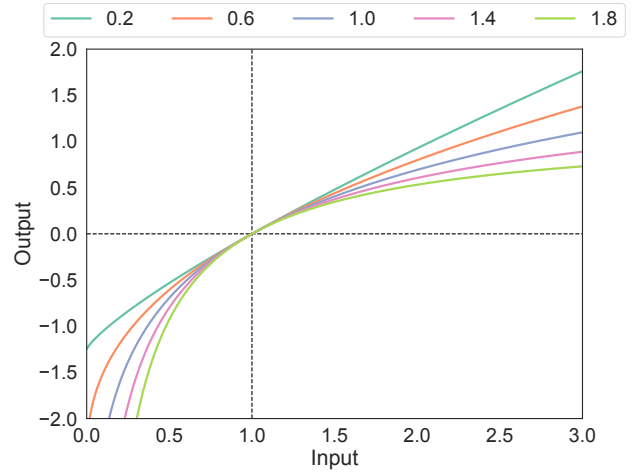


Fig. 2. Examples of q -logarithm with different q values: when $q > 0$, this function is regarded as a concave function; as can be seen in the intuitive, $\ln_{q+\epsilon}(x)$ with ϵ a positive small number is larger than $\ln_q(x)$.

In the case of the β -VAE [11], the second term is multiplied by $\beta \in (0, \infty)$, although its derivation is different from the above. By giving $\beta > 1$, the regularization to $p(\mathbf{z})$ is strengthened, and the role of each axis of the latent space, which has limited expressive ability, is clarified to perform the reconstruction of the inputs.

B. Tsallis statistics

Tsallis statistics refers to the organization of mathematical functions and associated probability distributions proposed by Tsallis [15]. It is organized based on q -deformed exponential and logarithmic functions, which are extensions of general exponential and logarithmic functions by a real number $q \in \mathbb{R}$. From Tsallis statistics, definitions essential in this paper are introduced below.

First, the q -logarithm, $\ln_q(x)$ with $x > 0$, is given as follows:

$$\ln_q(x) = \begin{cases} \ln(x) & q = 1 \\ \frac{x^{1-q} - 1}{1-q} & q \neq 1 \end{cases} \tag{3}$$

where q gives its shape as shown in Fig. 2. As can be seen in the figure, the q -logarithm with $q > 0$ is concave function. Note that when $q \rightarrow 1$, the lower equation converges to the natural logarithm.

In the q -logarithm, multiplication of two variables, $x, y > 0$, is no longer divided simply. That is, the following pseudo-additivity is derived.

$$\ln_q(xy) = \ln_q(x) + \ln_q(y) + (1-q) \ln_q(x) \ln_q(y) \tag{4}$$

Instead of the general multiplication, a new multiplication operation \otimes_q is introduced as follows [16]:

$$x \otimes_q y = \begin{cases} (x^{1-q} + y^{1-q} - 1)^{\frac{1}{1-q}} & x^{1-q} + y^{1-q} > 1 \\ 0 & \text{otherwise} \end{cases} \tag{5}$$

This definition means that the following additivity is satisfied when using \otimes_q .

$$\ln_q(x \otimes_q y) = \ln_q(x) + \ln_q(y) \tag{6}$$

By using \otimes_q , q -likelihood, which is maximized when the probability is given as q -Gaussian, can be defined with non i.i.d. data $X = \{\mathbf{x}_1, \dots, \mathbf{x}_N\}$ [16].

$$p(X) = p(\mathbf{x}_1) \otimes_q p(\mathbf{x}_2) \otimes_q \dots \otimes_q p(\mathbf{x}_N) \quad (7)$$

Finally, the deformed version of KL divergence named Tsallis divergence [17], KL_q , are introduced as follows:

$$\text{KL}_q(p_1 || p_2) = - \int p_1(x) \ln_q \frac{p_2(x)}{p_1(x)} dx \quad (8)$$

where p_1 and p_2 are arbitrary probability density functions. Since q -logarithm for all the x decreases as q increases, KL_q increases as q increases. Tsallis divergence can be derived by transformation of Renyi divergence, which has closed-form solutions for commonly-used distributions [18]. Hence, the q -VAE can be integrated with the different priors proposed in the previous work [19], [20].

III. Q-VARIATIONAL AUTOENCODER: Q-VAE

A. Derivation of ELBO

By combining eqs. (6) and (7), a new q -log likelihood to be maximized are derived. In addition, if $q > 0$, the q -logarithm is concave function (see Fig. 2), and therefore, Jensen's inequality can be used similar to eq. (1).

$$\begin{aligned} \ln_q p(X) &= \sum_{n=1}^N \ln_q \int p(\mathbf{x}_n | \mathbf{z}; \boldsymbol{\theta}) p(\mathbf{z}) d\mathbf{z} \\ &\geq \sum_{n=1}^N \mathbb{E}_{\rho(\mathbf{z}|\mathbf{x}_n; \boldsymbol{\phi})} \left[\ln_q \frac{p(\mathbf{x}_n | \mathbf{z}; \boldsymbol{\theta}) p(\mathbf{z})}{\rho(\mathbf{z} | \mathbf{x}_n; \boldsymbol{\phi})} \right] \\ &=: \mathcal{L}_q(X) \end{aligned} \quad (9)$$

Note again that X can be non i.i.d. data, unlike the log likelihood used in eq. (1).

According to eq. (4), $\mathcal{L}_q(X)$ can be divided into three terms and summarized to two terms similar to eq. (2).

$$\begin{aligned} \mathcal{L}_q(X) &= \sum_{n=1}^N \mathbb{E}_{\rho(\mathbf{z}|\mathbf{x}_n; \boldsymbol{\phi})} \left[\ln_q p(\mathbf{x}_n | \mathbf{z}; \boldsymbol{\theta}) \right. \\ &\quad \left. + \ln_q \frac{p(\mathbf{z})}{\rho(\mathbf{z} | \mathbf{x}_n; \boldsymbol{\phi})} \right. \\ &\quad \left. + (1-q) \ln_q p(\mathbf{x}_n | \mathbf{z}; \boldsymbol{\theta}) \ln_q \frac{p(\mathbf{z})}{\rho(\mathbf{z} | \mathbf{x}_n; \boldsymbol{\phi})} \right] \\ &= \sum_{n=1}^N \mathbb{E}_{\rho(\mathbf{z}|\mathbf{x}_n; \boldsymbol{\phi})} \left[\ln_q p(\mathbf{x}_n | \mathbf{z}; \boldsymbol{\theta}) \right. \\ &\quad \left. \times \left\{ 1 + (1-q) \ln_q \frac{p(\mathbf{z})}{\rho(\mathbf{z} | \mathbf{x}_n; \boldsymbol{\phi})} \right\} \right] \\ &\quad - \text{KL}_q(\rho(\mathbf{z} | \mathbf{x}_n; \boldsymbol{\phi}) || p(\mathbf{z})) \\ &\simeq \sum_{n=1}^N \ln_q p(\mathbf{x}_n | \mathbf{z}_n; \boldsymbol{\theta}) \left\{ 1 + (1-q) \ln_q \frac{p(\mathbf{z}_n)}{\rho(\mathbf{z}_n | \mathbf{x}_n; \boldsymbol{\phi})} \right\} \\ &\quad - \text{KL}_q(\rho(\mathbf{z} | \mathbf{x}_n; \boldsymbol{\phi}) || p(\mathbf{z})) \\ &= \sum_{n=1}^N \frac{\ln_q p(\mathbf{x}_n | \mathbf{z}_n; \boldsymbol{\theta})}{\beta_q(\mathbf{x}_n, \mathbf{z}_n)} - \text{KL}_q(\rho(\mathbf{z} | \mathbf{x}_n; \boldsymbol{\phi}) || p(\mathbf{z})) \end{aligned} \quad (10)$$

The first term is denotes the negative reconstruction error with a new coefficient $1/\beta_q(\mathbf{x}_n, \mathbf{z}_n)$ and the second term, i.e., Tsallis divergence between the posterior and the prior, is the regularization term to try to $\mathbf{z} \sim p(\mathbf{z})$.

Here, three practical remarks are given. The probability outputted from the decoder $p(\mathbf{x} | \mathbf{z}; \boldsymbol{\theta})$ should be assumed as q -Gaussian (or Bernoulli distribution for binary inputs) to match the reconstruction error term with that of the normal VAE. The computational graph of $\beta_q(\mathbf{x}, \mathbf{z})$ is cut to simplify backpropagation and to regard it merely as the coefficient. Tsallis divergence of Gaussian has a closed-form solution, as derived in the literature [17], [18]. Given p_1 and p_2 as d -dimensional normal distribution with parameters $\boldsymbol{\mu}_1, \Sigma_1, \boldsymbol{\mu}_2$, and Σ_2 , respectively, it is solved as follows:

$$\text{KL}_q(p_1 || p_2) = \begin{cases} \frac{1}{2} \left\{ \text{tr}(\Sigma_2^{-1} \Sigma_1) + \ln \frac{|\Sigma_2|}{|\Sigma_1|} - d \right. \\ \quad \left. + (\boldsymbol{\mu}_2 - \boldsymbol{\mu}_1)^\top \Sigma_2^{-1} (\boldsymbol{\mu}_2 - \boldsymbol{\mu}_1) \right\} & q = 1 \\ \frac{\exp(\frac{1}{2} I_q(p_1 || p_2)) - 1}{q-1} & q \neq 1 \end{cases} \quad (11)$$

where,

$$\begin{aligned} I_q(p_1 || p_2) &= \ln \frac{|\Sigma_2|^q |\Sigma_1|^{1-q}}{|\Sigma|} \\ &\quad + q(1-q) (\boldsymbol{\mu}_2 - \boldsymbol{\mu}_1)^\top \Sigma^{-1} (\boldsymbol{\mu}_2 - \boldsymbol{\mu}_1) \end{aligned} \quad (12)$$

$$\Sigma = q \Sigma_2 + (1-q) \Sigma_1 \quad (13)$$

B. Analysis

In the q -VAE, the above ELBO is maximized by optimizing the parameters $\boldsymbol{\theta}$ of the decoder and $\boldsymbol{\phi}$ of the encoder. As can be seen in eqs. (2) and (10), the q -VAE is the extension of the normal VAE by adding the parameter q since \ln_q, β_q , and KL_q converge on $\ln, 1$, and KL , respectively if $q \rightarrow 1$.

In addition, the q -VAE can be regarded as a kind of the β -VAE with an adaptive $\beta_q(\mathbf{x}_n, \mathbf{z}_n)$. According to range of q , its behaviors can be divided into three cases:

- 1) $q = 1$: As mentioned the above, β_q is always equal to 1 in this case. This case is therefore regarded as the normal VAE or the β -VAE with an additional hyperparameter β .
- 2) $q < 1$: In general, the posterior $\rho(\mathbf{z}_n | \mathbf{x}_n; \boldsymbol{\phi})$ contains more information than the prior $p(\mathbf{z}_n)$. Hence, β_q would probably be larger 1. That is, the posterior is strongly constrained to discard the information about the inputs only when it has much information, and consequently, only essential information of the inputs would be expected to be left without duplication in the latent space (and its axes). Note however that smaller q leads to smaller KL_q , hence, if q is too small, no matter how large β_q is, the constraint to the prior would not work as described the above since it is originally small.
- 3) $q > 1$: In contrast to the case with $q < 1$, β_q would probably be smaller than 1. That is, the reconstruction would be prioritized without the constraint to the prior. In addition, as can be seen in eq. (13), the covariance matrix for the Tsallis divergence calculation is likely to violate its positive-semidefinite condition.

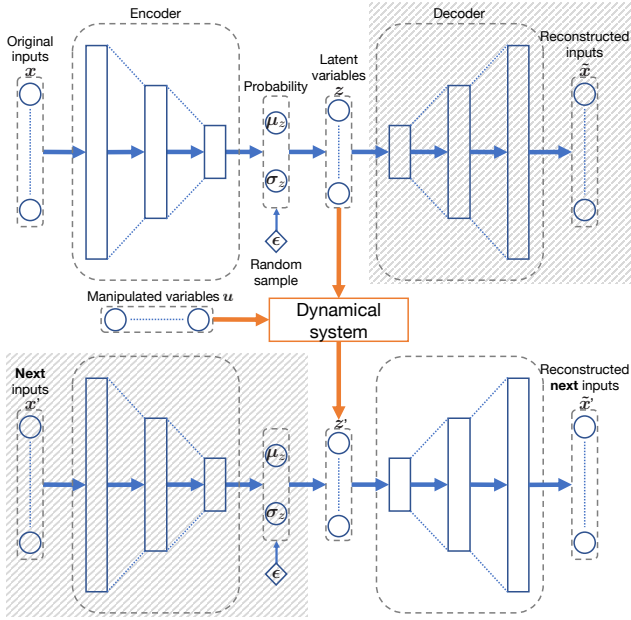


Fig. 3. Dynamics model in latent space: the next inputs \mathbf{x}' is predicted according to the current inputs \mathbf{x} and the given manipulated variables \mathbf{u} ; in this paper, a dynamical system is given to be time-varying linear and diagonal.

From the above, we can expect that q smaller than 1 is better to achieve the disentangled representation learning with stable computation. To the best of my knowledge, no methods for automatically tuning β in the β -VAE has not been proposed so far. This method, named the q -VAE, is therefore the first method that tunes β by mathematically natural derivation.

To avoid the adverse effects caused by too small q , the simplified version is additionally investigated in this paper.

$$\mathcal{L}_q^{\text{smp}}(X) = \sum_{n=1}^N \frac{\ln_q p(\mathbf{x}_n | \mathbf{z}_n; \boldsymbol{\theta})}{\beta_q(\mathbf{x}_n, \mathbf{z}_n)} - \text{KL}(\rho(\mathbf{z} | \mathbf{x}_n; \boldsymbol{\phi}) || p(\mathbf{z})) \quad (14)$$

That means, KL instead of KL_q is employed. When $q < 1$, $\mathcal{L}_q^{\text{smp}}$ is smaller than the original \mathcal{L}_q since KL is stronger than KL_q . Even though this case would avoid too weak constraint by KL_q with $q \ll 1$, however, it has a risk to make the constraint stronger when $q \simeq 1$.

C. Extension to latent dynamical systems

The another advantage from Tsallis statistics is the q -likelihood defined in eq. (7). Its q -logarithm can be converted to the sum of q -log likelihoods of respective samples without independency (precisely, with q -independency) between each sample. That is, even if the inputs are sampled from dynamical systems with a transition probability, the q -VAE would be applied as it is.

A simple dynamical system is designed in reference to the literature [8], [21] (also see Fig. 3). Specifically, a trajectory of the inputs $X = \{\mathbf{x}_1, \dots, \mathbf{x}_t, \dots, \mathbf{x}_T\}$ with T the maximum time step, is generated from the following

dynamics with parameters $\boldsymbol{\eta}$:

$$\mathbf{z}_t \sim \rho(\mathbf{z}_t | \mathbf{x}_t; \boldsymbol{\phi}) \quad (15)$$

$$\mathbf{z}_{t+1} \sim p(\mathbf{z}_{t+1} | \mathbf{z}_t, \mathbf{u}_t; \boldsymbol{\eta}) \quad (16)$$

$$\mathbf{x}_{t+1} \sim p(\mathbf{x}_{t+1} | \mathbf{z}_{t+1}; \boldsymbol{\theta}) \quad (17)$$

where \mathbf{u} denotes the manipulated variables of the dynamical system. In this paper, \mathbf{u}_t is given randomly or by experts.

In that time, $\mathcal{L}_q(X)$ in eq. (10) is redefined as follows:

$$\mathcal{L}_q^{\text{dyn}}(X) = \sum_{t=1}^T \frac{\ln_q p(\mathbf{x}_{t+1} | \mathbf{z}_{t+1}^\eta; \boldsymbol{\theta})}{\beta_q(\mathbf{x}_t, \mathbf{z}_t)} - \text{KL}(\rho(\mathbf{z} | \mathbf{x}_t; \boldsymbol{\phi}) || p(\mathbf{z})) \quad (18)$$

where \mathbf{z}_{t+1}^η denotes \mathbf{z}_{t+1} predicted by the latent dynamics.

When minimizing this, $\boldsymbol{\eta}$ also be optimized implicitly. The information about the dynamics, however, would penetrate into the decoder (and the encoder), and $\boldsymbol{\eta}$ would fail to represent the latent dynamics. Therefore, to distinguish the functions of encoder, dynamics, and decoder, the following function is additionally maximized with γ weight.

$$\mathcal{L}_q^{\text{latent}}(X) = \gamma \sum_{t=1}^T \ln \rho(\mathbf{z}_{t+1}^\eta | \mathbf{x}_{t+1}; \boldsymbol{\phi}) \quad (19)$$

This is given from the similar concept of the previous work [8], but this can be used even if only the sampled latent variables can be transitioned to the next ones.

Now, the general form of the latent dynamics is simplified as much as possible to reduce computational cost. The general (i.e., nonlinear) dynamics is regarded as time-varying linear one, as used in general nonlinear control via first-order Taylor expansion. As mentioned before, the q -VAE is suitable for the disentangled representation, and therefore, the latent variables are ideally independent on each other. In total, the latent dynamics is simplified as follows:

$$\mathbf{z}_{t+1} = \text{diag}(\mathbf{a}(\mathbf{z}_t; \boldsymbol{\eta}))\mathbf{z}_t + B(\mathbf{z}_t; \boldsymbol{\eta})\mathbf{u}_t \quad (20)$$

where \mathbf{a} and B are the outputs of the network with the inputs \mathbf{z} and the parameters $\boldsymbol{\eta}$. Actually, this design of the latent dynamics would cause modeling error unless the latent variables are encoded to match this by the disentangled representation learning.

IV. MNIST BENCHMARK

First, the performance of the disentangled representation by the q -VAE is verified. As a dataset, MNIST, which contains $28 \times 28 = 784$ -dimensional images with handwritten numbers 0 ~ 9, is used.

A. Criteria of disentangled representation

To evaluate how the latent space obtains the disentangled representation, the fact that the disentangled representation aims to gain the independent axes with essential information is paid attention. Its concept is closely related to an independent component analysis (ICA) [22]. Hence, as a criterion of the disentangled representation, a kurtosis in the latent space is employed according to the ICA.

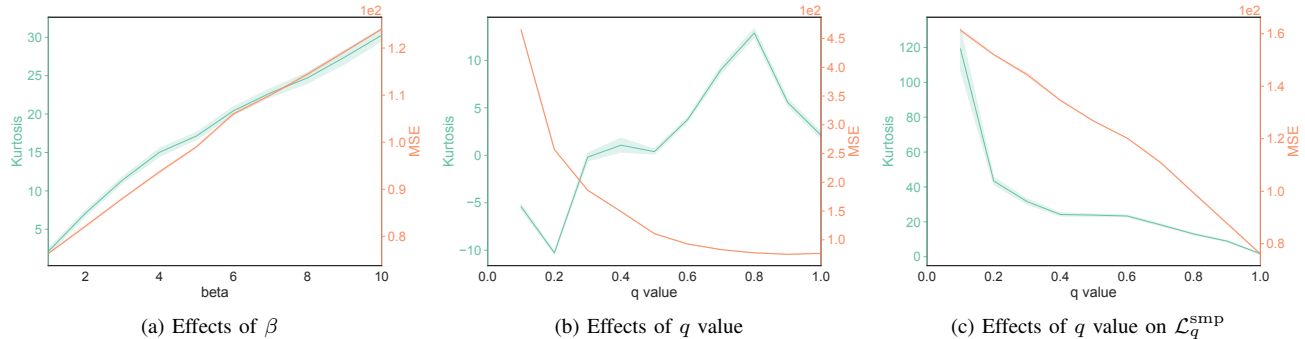


Fig. 4. Criteria with respect to hyperparameters: (a) both kurtosis and BCE were increased almost linearly as β gets large; that is, a tradeoff between the disentangled representation and the reconstruction abilities would be inevitable in the β -VAE; (b) the BCE was inversely proportional to q value, while the kurtosis got unimodal-like shape; in (c), the simplified q-VAE defined in eq. (14), showed that both the kurtosis and BCE are inversely proportional to q value.

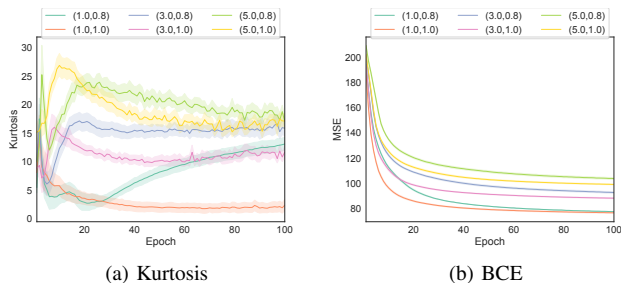


Fig. 5. Learning curves of the (β, q) -VAEs: note that, the β -VAE and the proposed q-VAE can be combined without any conflicts; the β -VAE was effective to acquire the large kurtosis, but it was at the expense of the BCE; the q-VAE not only increased the kurtosis but also suppressed the deterioration of the BCE.

Specifically, the kurtosis from the sampled data $Z = \{z_1, \dots, z_N\}$ where $z_n \sim \rho(z | x_n; \phi)$, κ , is defined as Mardia’s kurtosis [23]:

$$\kappa = \frac{1}{N} \sum_{n=1}^N \left\{ (z_n - \mu_z)^\top \Sigma_z^{-1} (z_n - \mu_z) \right\} - d(d+2) \quad (21)$$

where μ_z and Σ_z denote the mean and covariance of Z , respectively. The larger κ means the better disentangled representation.

As another criterion, the reconstruction error is important to show how much the appropriate latent space is achieved. Therefore, a binary cross entropy (BCE) is employed. The smaller BCE means the better reconstruction.

B. Network structure

The q-VAE gives the different ELBO (i.e., the loss function), hence, the same network structure is constructed for all the methods compared. Note that the networks are constructed by using PyTorch [24].

The images are converted into the 784-dimensional inputs. The encoder has five full-connected layers: 500 neurons; 275 neurons; 50 neurons; and 20 neurons corresponding to μ and σ of the posterior (i.e., $d = 10$). The decoder also has five full-connected layers: 255 neurons; 500 neurons; and 784 neurons corresponding to the reconstructed inputs.

The outputs from the intermediate layers of both the encoder and the decoder go through layer normalization [25] and Swish functions [26], [27]. As remarks, it is found that the appropriate normalization techniques like the layer normalization would be important to reduce the variance of kurtosis. The activation function used in the intermediate layers would improve only the BCE.

C. Results

First, the effects of β in the β -VAE [11] and q value are investigated. That is, (a) $\beta = [1, 10]$ with 1 increment and (b) $q = [0.1, 1]$ with 0.1 increment are tested 50 trials with 100 epochs, and Figs. 4(a) and (b) are plotted from them, respectively. Note that random seeds in respective trials are given as the number of trials.

As expected, the β -VAE could increase the kurtosis (i.e., the disentangled representation ability) as β got large (see Fig. 4(a)). The BCE was however deteriorated linearly along with that. Namely, the β -VAE has a problem of tradeoff between the disentangled representation and reconstruction abilities, which may make the design of β difficult.

In contrast, as can be seen in Fig. 4(b), the kurtosis has a peak on $q = 0.8$, while the BCE was monotonically decreased as q value increased. In addition, since the BCEs in the cases with $q > 0.7$ seemed to be small sufficiently, it is suggested that q value is desired to be around 0.8 to achieve both the disentangled representation and reconstruction abilities. In other words, they are achieved by the q-VAE with simple implementation, a slight increase of computational cost, and a small effort for optimization of hyperparameters. Only one concern is that the small q value makes Tsallis divergence KL_q small and deteriorates the reconstruction accuracy by increasing βq .

The results with eq. (14), which is proposed to avoid such behavior, is additionally shown in Fig. 4(c). Due to stronger and stable constraint to the prior, the kurtosis was extremely increased as q decreased. As expected, however, the stronger constraint caused the increase of BCE even in $q \simeq 1$. That is, the tradeoff as well as that of the β -VAE appeared, hence, the original derivation in eq. (10) is desired rather than the simplified version in eq. (14).

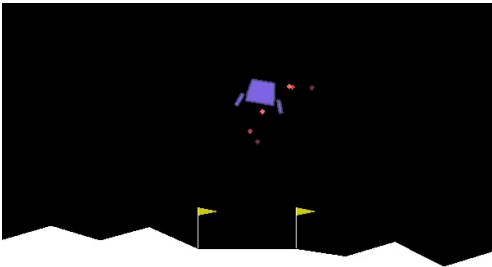


Fig. 6. LunarLanderContinuous-v2 [28]: a lander aims to safely land inside two flags by controlling a main engine and two side engines; it has eight-dimensional state and three-dimensional action spaces.

Next, the q-VAE is combined with the β -VAE. Learning curves of several combinations are depicted in Fig. 5, where tuples denote (β, q) . The q-VAE and the β -VAE seemed not to have any interferences with each other. By focusing on the pairs of i) the (1.0, 0.8)- and (3.0, 1.0)-VAEs and ii) the (3.0, 0.8)- and (5.0, 1.0)-VAEs, it is found that the q-VAE could increase the kurtosis as much as the β -VAE, while maintaining the BCE rather than the β -VAE. In particular, the (1.0, 0.8)-VAE achieved the superior performance of the disentangled representation ability to the (3.0, 1.0)-VAE, while also achieving the similar performance of the reconstruction ability to the (1.0, 1.0)-VAE.

V. LEARNING OF LATENT DYNAMICS

A. Dataset

As a proof of concept, a dynamical simulation provided by Open AI Gym [28], named LunarLanderContinuous-v2 (see Fig. 6), is learned by the q-VAE with eqs. (18)–(20). It observes eight-dimensional state space data, and is controlled via three-dimensional action space. An expert controls a lander to safely land it on the permitted area via a keyboard interface. In that time, the pairs of state and action are collected as a non i.i.d. expert’s trajectory data. A dataset totally consists of 150 trajectories for train (and validation) and 50 trajectories for test. All the tuples (s_t, a_t, s_{t+1}) in the 150 trajectories is divided into 80 % train data and 20 % validation. During validation (after each epoch of train), only the error of state prediction is evaluated for checking under/over fitting. After the end of train, respective methods try to predict the state (and latent variables) trajectories for evaluation of them.

In this experiment, the prediction errors are the main concern to show that the q-VAE is suitable to extract latent dynamics, which is useful to reduce computational cost of like nonlinear model predictive control (MPC) [29], [30]. Hence, a mean squared error (MSE) between the predicted state and the true one (or the predicted and encoded latent variables). In addition, when applying the learned model to like MPC, long-term prediction is more important, and therefore, all the states (and latent variables) are predicted from the initial state by repeatedly going through the latent dynamics. Totally, four types of MSEs are given: 1-step state;

TABLE I
NETWORK DESIGNS FOR LEARNING OF LATENT DYNAMICS

Version	Encoder	Latent dynamics
V1	[500, 400, 300, 200, 100]	[100, 100, 100, 100, 100]
V2	[250, 200, 150, 100]	[50, 50, 50]
V3	[100, 100, 100]	[100, 100, 100]

1-step latent; T -step state; and T -step latent. Note that each trajectory has about 500 steps, hence the q-VAE is required to predict the states from one to about 500 steps future only by the initial state and actions at respective times.

B. Network structure

Due to real number inputs, all the layers are given to be fully connected. In this paper, three types of network structures are prepared to show network-invariant performance. The numbers of neurons for their layers are listed in Table I: the V1 is the largest structure; the V2 is with moderate encoder and the smallest latent dynamics; and the V3 is the simplest design. Note that a decoder inverts the hidden layers in the encoder with different parameters. As well as the MNIST benchmark, layer normalization [25] and Swish functions [26], [27] are employed.

C. Results

Three conditions with different (β, q) are compared: (0.0, 1.0) to show that the standard autoencoder does not have continuity in the latent space; (0.01, 1.0) as baseline; and (0.01, 0.8) as the proposed q-VAE. Here, β is smaller than the case of MNIST since the ratio between input and latent dimensions are about 100 times different. As common conditions, three dimensional latent space is given, and γ in eq. (19) is set as 0.1. For each condition, 50 trials with different random seeds are conducted, and the mean of the prediction error during each trajectory is regarded as a score.

All the scores are summarized in Fig. 7. Regardless of the conditions and network structures, the ability to predict 1-step state and latent variables was achieved. In contrast, T -step prediction showed us the superiority of the q-VAE. For T -step latent variables prediction, the q-VAE yielded the stable scores, although the other methods made it sometime diverge. This implies that the latent space extracted by the q-VAE has natural representation of dynamics. As a result, T -step state prediction was improved by the q-VAE. Interestingly, although the other methods with the largest network structure (i.e., the V1) gained the better scores than the other structures, the q-VAE achieved the same excellent prediction performance regardless of the network structure.

VI. CONCLUSION

This paper proposed a novel VAE derived according to Tsallis statistics, named q-VAE. Thanks to Tsallis statistics, the q-VAE gained mainly three features: i) an adaptive β_q according to the amount of information in the latent space; ii) Tsallis divergence regularization instead of the standard KL divergence one; and iii) release from the assumption of i.i.d. input data. First two features are suitable for disentangled

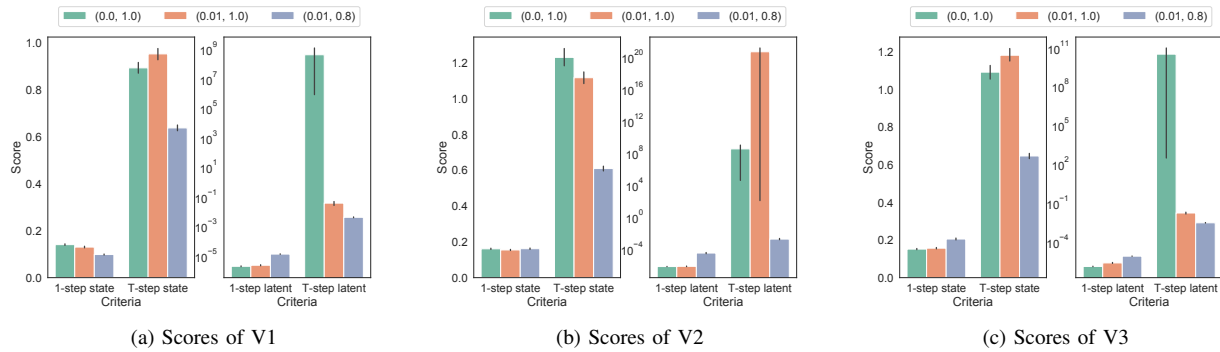


Fig. 7. Scores for prediction error: all the methods succeeded in 1-step prediction with the same level; in all the cases, the q-VAE gained the better T -step prediction than the others; In particular, the other methods made the T -step latent sometimes diverge, but the q-VAE did not.

representation learning, and indeed, the q-VAE achieved the better performance than the baseline, β -VAE, in MNIST benchmark. In addition, the importance of second feature, using Tsallis divergence, was verified by testing the simplified version of the q-VAE. Third feature enables us to use the q-VAE for learning of latent dynamics from non i.i.d. data. As a proof of concept, the q-VAE succeeded in stably and accurately predicting the (about 500 steps) future states only from the initial state and actions at respective times.

Future work of this study is to apply the q-VAE to real complex systems with high-dimensional input like a vision, and to control them from the prediction of future states in real time using latest control theory.

REFERENCES

- [1] Y. LeCun, Y. Bengio, and G. Hinton, "Deep learning," *nature*, vol. 521, no. 7553, p. 436, 2015.
- [2] D. Kalashnikov, A. Irpan, P. Pastor, J. Ibarz, A. Herzog, E. Jang, D. Quillen, E. Holly, M. Kalakrishnan, V. Vanhoucke, *et al.*, "Scalable deep reinforcement learning for vision-based robotic manipulation," in *Conference on Robot Learning*, 2018, pp. 651–673.
- [3] Y. Tsurumine, Y. Cui, E. Uchibe, and T. Matsubara, "Deep reinforcement learning with smooth policy update: Application to robotic cloth manipulation," *Robotics and Autonomous Systems*, vol. 112, pp. 72–83, 2019.
- [4] D. P. Kingma and M. Welling, "Auto-encoding variational bayes," in *International Conference on Learning Representations*, 2014.
- [5] T. Kobayashi, T. Aoyama, K. Sekiyama, and T. Fukuda, "Selection algorithm for locomotion based on the evaluation of falling risk," *IEEE Transactions on Robotics*, vol. 31, no. 3, pp. 750–765, 2015.
- [6] M. Neunert, C. De Crousaz, F. Furrer, M. Kamel, F. Farshidian, R. Siegwart, and J. Buchli, "Fast nonlinear model predictive control for unified trajectory optimization and tracking," in *IEEE international conference on robotics and automation*. IEEE, 2016, pp. 1398–1404.
- [7] T. Kobayashi, K. Sekiyama, Y. Hasegawa, T. Aoyama, and T. Fukuda, "Unified bipedal gait for autonomous transition between walking and running in pursuit of energy minimization," *Robotics and Autonomous Systems*, vol. 103, pp. 27–41, 2018.
- [8] M. Watter, J. Springenberg, J. Boedecker, and M. Riedmiller, "Embed to control: A locally linear latent dynamics model for control from raw images," in *Advances in neural information processing systems*, 2015, pp. 2746–2754.
- [9] M. Fraccaro, S. Kamronn, U. Paquet, and O. Winther, "A disentangled recognition and nonlinear dynamics model for unsupervised learning," in *Advances in Neural Information Processing Systems*, 2017, pp. 3601–3610.
- [10] I. Higgins, D. Amos, D. Pfau, S. Racaniere, L. Matthey, D. Rezende, and A. Lerchner, "Towards a definition of disentangled representations," *arXiv preprint arXiv:1812.02230*, 2018.
- [11] I. Higgins, L. Matthey, A. Pal, C. Burgess, X. Glorot, M. Botvinick, S. Mohamed, and A. Lerchner, "beta-vae: Learning basic visual concepts with a constrained variational framework," in *International Conference on Learning Representations*, 2017.
- [12] C. P. Burgess, I. Higgins, A. Pal, L. Matthey, N. Watters, G. Desjardins, and A. Lerchner, "Understanding disentangling in β -vae," *arXiv preprint arXiv:1804.03599*, 2018.
- [13] T. Q. Chen, X. Li, R. B. Grosse, and D. K. Duvenaud, "Isolating sources of disentanglement in variational autoencoders," in *Advances in Neural Information Processing Systems*, 2018, pp. 2610–2620.
- [14] H. Kim and A. Mnih, "Disentangling by factorising," in *International Conference on Machine Learning*, 2018, pp. 2654–2663.
- [15] C. Tsallis, "Possible generalization of boltzmann-gibbs statistics," *Journal of statistical physics*, vol. 52, no. 1-2, pp. 479–487, 1988.
- [16] H. Suyari and M. Tsukada, "Law of error in tsallis statistics," *IEEE Transactions on Information Theory*, vol. 51, no. 2, pp. 753–757, 2005.
- [17] F. Nielsen and R. Nock, "A closed-form expression for the sharma-mittal entropy of exponential families," *Journal of Physics A: Mathematical and Theoretical*, vol. 45, no. 3, p. 032003, 2011.
- [18] M. Gil, F. Alajaji, and T. Linder, "Rényi divergence measures for commonly used univariate continuous distributions," *Information Sciences*, vol. 249, pp. 124–131, 2013.
- [19] E. Jang, S. Gu, and B. Poole, "Categorical reparameterization with gumbel-softmax," *arXiv preprint arXiv:1611.01144*, 2016.
- [20] T. Kobayashi, "Variational deep embedding with regularized student-t mixture model," in *International Conference on Artificial Neural Networks*. Springer, 2019, pp. 443–455.
- [21] M. Karl, M. Soelch, J. Bayer, and P. van der Smagt, "Deep variational bayes filters: Unsupervised learning of state space models from raw data," in *International Conference on Learning Representations*, 2017.
- [22] M. Girolami and C. Fyfe, "Negentropy and kurtosis as projection pursuit indices provide generalised ica algorithms," in *Advances in Neural Information Processing Systems Workshop*, vol. 9, 1996.
- [23] K. V. Mardia, "Measures of multivariate skewness and kurtosis with applications," *Biometrika*, vol. 57, no. 3, pp. 519–530, 1970.
- [24] A. Paszke, S. Gross, S. Chintala, G. Chanan, E. Yang, Z. DeVito, Z. Lin, A. Desmaison, L. Antiga, and A. Lerer, "Automatic differentiation in pytorch," in *Advances in Neural Information Processing Systems Workshop*, 2017.
- [25] J. L. Ba, J. R. Kiros, and G. E. Hinton, "Layer normalization," *arXiv preprint arXiv:1607.06450*, 2016.
- [26] P. Ramachandran, B. Zoph, and Q. V. Le, "Searching for activation functions," *arXiv preprint arXiv:1710.05941*, 2017.
- [27] S. Elfving, E. Uchibe, and K. Doya, "Sigmoid-weighted linear units for neural network function approximation in reinforcement learning," *Neural Networks*, vol. 107, pp. 3–11, 2018.
- [28] G. Brockman, V. Cheung, L. Pettersson, J. Schneider, J. Schulman, J. Tang, and W. Zaremba, "Openai gym," *arXiv preprint arXiv:1606.01540*, 2016.
- [29] J. Koenemann, A. Del Prete, Y. Tassa, E. Todorov, O. Stasse, M. Bennewitz, and N. Mansard, "Whole-body model-predictive control applied to the hrp-2 humanoid," in *IEEE/RSJ International Conference on Intelligent Robots and Systems*. IEEE, 2015, pp. 3346–3351.
- [30] B. Amos, I. Jimenez, J. Sacks, B. Boots, and J. Z. Kolter, "Differentiable mpc for end-to-end planning and control," in *Advances in Neural Information Processing Systems*, 2018, pp. 8289–8300.